

AD-A129 465

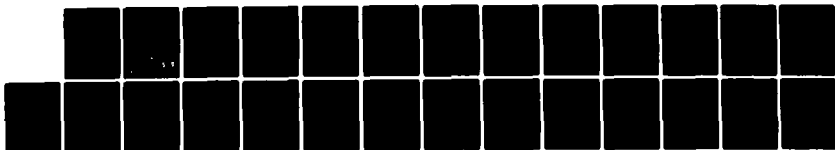
CHARGE-CHARGE CORRELATION FUNCTIONS IN ULTRA DENSE
PLASMAS(U) NAVAL RESEARCH LAB WASHINGTON DC
R CAUBLE ET AL. 22 JUN 83 NRL-MR-5104

1/1

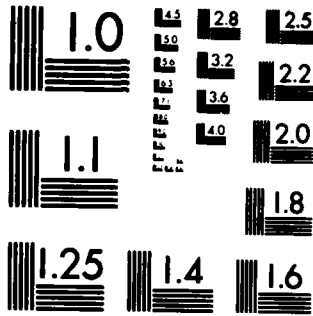
UNCLASSIFIED

F/G 20/9

NL



END
DATE
FILMED
7 83
DTIC



MICROCOPY RESOLUTION TEST CHART
NATIONAL BUREAU OF STANDARDS-1963-A

(2)

NRL Memorandum Report 5104

AD A129465

Charge-Charge Correlation Functions in Ultra Dense Plasmas

R. CAUBLE,* D. B. BOERCKER,** AND P. KEPPLER

*Plasma Radiation Branch
Plasma Physics Division*

**Berkeley Research Associates
Springfield, VA 22151*

***University of California
Lawrence Livermore National Laboratory
Livermore, CA 94550*

June 22, 1983

This work was supported in part by the Office of Naval Research.



NAVAL RESEARCH LABORATORY
Washington, D.C.

DTIC
ELECTE
JUN 17 1983
S E D

Approved for public release; distribution unlimited.

DTIC FILE COPY

83 06 17 051

20. ABSTRACT (Continued)

cont → short-range quantum effects. The results are compared with molecular dynamics simulations of the plasma using the effective pair potential and with a hierarchial approach involving known sum rules. ↗

CONTENTS

I. Introduction 1

II. Kinetic Equation 3

III. The Collision Models 6

IV. Discussion 19

Acknowledgments 20

References 21

Accession For	
NTIS GRA&I	<input checked="" type="checkbox"/>
DTIC TAB	<input type="checkbox"/>
Unannounced	<input type="checkbox"/>
Justification	
By _____	
Distribution/	
Availability Codes	
Dist	Avail and/or Special
A	



CHARGE-CHARGE CORRELATION FUNCTIONS IN ULTRA DENSE PLASMAS

I. INTRODUCTION

Theoretical investigations into the properties of dense plasmas have benefitted greatly from the results of computer simulations of model systems. The simplest of these models is the classical one-component plasma (OCP) which is a system of classical ions imbedded in a uniform neutralizing background. Monte Carlo^{1,2} and molecular dynamics³ simulations of the OCP have guided theoretical pursuits and have provided benchmarks for analytic calculations of its properties, which are now well understood.^{4,5}

The OCP is, however, a very simplified model of a real plasma and is applicable only to systems which are so dense that the electrons are completely degenerate. When the electrons are non-degenerate, they can no longer be pictured as a uniform, rigid background, and the OCP becomes an inappropriate model. Under these conditions, one must treat both the electrons and ions as particles. A reasonable model which does this is the two-component plasma (TCP).

In the TCP the electrons and ions are treated as classical (quasi-) particles that interact through effective potentials which deviate from pure Coulombic behavior at short distances in a way that simulates the essential quantum diffraction effects. A specific form for such a potential is the one suggested by Deutsch.⁶ If α and β are species labels, and if

$$\chi_{\alpha\beta} \equiv h/(2\pi\mu_{\alpha\beta}k_B T)^{1/2}$$

where $\mu_{\alpha\beta}$ is the reduced mass of this interacting pair, then Deutsch's potential is

$$v_{\alpha\beta}(r) = \frac{Z_\alpha Z_\beta e^2}{r} [1 - \exp(-r/\chi_{\alpha\beta})] . \quad (1)$$

This potential remains finite at the origin, and, therefore, prevents the collapse of the system. It is expected to give reasonable results for non-degenerate plasmas with temperatures above the ionization potential and

Manuscript approved April 8, 1983.

coupling parameters less than about two, or

$$\Gamma = \frac{\beta e^2}{a} \lesssim 2$$

where $a^3 = 3/4\pi n = r_s^3 a_0^3$ and a_0 is the Bohr radius.

The TCP is more difficult to simulate than the OCP, but recently Hansen and McDonald^{7,8} have published results of molecular dynamics (MD) analyses of a fully ionized hydrogen TCP using the effective potential in Eq. (1). Among the properties calculated from the simulation data is the dynamic charge-charge structure factor $S_{QQ}(k, \omega)$. As the Fourier transform of the charge density-charge density time correlation function, $S_{QQ}(k, \omega)$ reflects in its shape the spectrum of longitudinal modes in the plasma. The motivation of this paper is to use the simulation data of Ref. 8 as a reference against which various kinetic theoretical calculations of $S_{QQ}(k, \omega)$ can be tested. A similar study⁹ has already been made for the OCP; the intention here is to generalize that work to two components.

The types of theories of interest here are microscopic theories based upon formally exact kinetic equations derived from projection operator¹⁰⁻¹² or other techniques.¹³⁻¹⁶ A general characteristic of such theories is the separation of the so-called "memory" operator into a static mean-field or Vlasov term and a frequency dependent collision term. Calculations of density fluctuations in dense plasmas, using just such a theory, were performed several years ago by Linnebur and Duderstadt.¹⁷ Unfortunately, they were unable to estimate the short-range part of the direct correlation functions appearing in the memory operator and had to approximate those correlations by their Debye-Huckel limits. We are now able to calculate the direct correlation functions using the potential in Eq. (1) in the so-called hypernetted chain (HNC) equation.^{18,19} This is an approximate integral equation method for calculating static correlation functions which has proven to be accurate for plasmas in which the coupling parameter is of order unity⁴, and produces excellent agreement with the static properties calculated by computer simulations in Ref. 8. The proposal here, then, is to generate the HNC direct correlation functions and use them in the model kinetic theories described in Ref. 17.

In Section II, we define the quantities of interest and review the

basic kinetic theory concepts involved. Calculations based upon three different collision models are presented in Section III, and in Section IV we present our conclusions.

II. KINETIC EQUATION

For a hydrogen plasma the dynamic charge-charge structure factor is defined by

$$S_{QQ}(k, \omega) = \frac{e^2}{2} [S_{ii}(k, \omega) - 2S_{ei}(k, \omega) + S_{ee}(k, \omega)] , \quad (2)$$

where the partial density correlation functions $S_{\alpha\beta}(k, \omega)$ with $\alpha, \beta = i, e$ are given by

$$S_{\alpha\beta}(k, \omega) = \int d^3p d^3p' \frac{1}{2\pi} \int dt e^{i\omega t} \frac{1}{N} \langle f_{\alpha}(\vec{k} \vec{p} t) f_{\beta}(-\vec{k} \vec{p}' t) \rangle \quad (3)$$

$$\equiv \int d^3p d^3p' \int dt e^{i\omega t} S_{\alpha\beta}(kt; \vec{p} \vec{p}') .$$

Here

$$f_{\alpha}(\vec{k} \vec{p} t) = \int d^3r e^{-i\vec{k} \cdot \vec{r}} f_{\alpha}(\vec{r} \vec{p} t) \quad (4)$$

is the Fourier transform of the phase-space density

$$f_{\alpha}(\vec{r} \vec{p} t) = \sum_{j=1}^N \delta(\vec{r} - \vec{r}_j^{\alpha}(t)) \delta(\vec{p} - \vec{p}_j^{\alpha}(t)) . \quad (5)$$

In Eq. (3), N is the number of ions in the system and brackets indicate an average over the equilibrium ensemble. It is not customary to calculate $S_{\alpha\beta}(k, \omega)$ directly, but rather to find it from

$$S_{\alpha\beta}(k, \omega) = 2 \operatorname{Re} \int d^3p d^3p' \check{S}_{\alpha\beta}(kz; \vec{p} \vec{p}') , \quad (6)$$

where the Laplace transform function $\check{S}_{\alpha\beta}(kz; \vec{p} \vec{p}')$ is

$$\tilde{S}_{\alpha\beta}(kz; \vec{p}\vec{p}') = \int_0^\infty dt e^{izt} S_{\alpha\beta}(kt; \vec{p}\vec{p}') . \quad (7)$$

The advantage is that the functions $\tilde{S}_{\alpha\beta}$ can be found from the solution to a coupled set of kinetic equations of the form ¹⁷

$$\left(z - \frac{\vec{p} \cdot \vec{k}}{m_\alpha}\right) \tilde{S}_{\alpha\beta}(kz; \vec{p}\vec{p}') + \frac{\vec{p} \cdot \vec{k}}{m_\alpha} M_\alpha(p) \sum_{\gamma=e,i} c_{\alpha\gamma}(k) \int d^3 p'' \tilde{S}_{\gamma\beta}(kz; \vec{p}''\vec{p}') \quad (8)$$

$$- \sum_{\gamma=e,i} \int d^3 p'' \phi_{\alpha\gamma}(kz; \vec{p}\vec{p}'') \tilde{S}_{\gamma\beta}(kz; \vec{p}''\vec{p}') = i S_{\alpha\beta}(k, t=0; \vec{p}\vec{p}') .$$

In Eq. (8), $M_\alpha(p)$ represents the Maxwell-Boltzmann distribution function (normalized to unity), and the $c_{\alpha\beta}$'s are the direct correlation functions defined by the Ornstein-Zernike relations

$$c_{\alpha\beta}(k) = h_{\alpha\beta}(k) - \sum_{\gamma=e,i} c_{\alpha\gamma}(k) h_{\gamma\beta}(k) , \quad (9)$$

where

$$h_{\alpha\beta}(k) = S_{\alpha\beta}(k) - \delta_{\alpha\beta} \quad (10)$$

and

$$S_{\alpha\beta}(k) = \int d^3 p d^3 p' S_{\alpha\beta}(k, t=0; \vec{p}\vec{p}') \quad (11)$$

is the static partial structure factor for species α and β . (Note that in Eq. (9) and Eq. (10) a factor of density has been absorbed into the usual definitions). The effects of collisions are contained in the operators $\phi_{\alpha\beta}(kz; \vec{p}\vec{p}')$. Formally exact expressions exist for these operators, but they will not be presented here. Instead, we will simply present results based upon various models for them.

Before preceding we note for future convenience that, in analogy with the single species case¹³, Eq. (8) can be solved formally to obtain the Laplace transformed functions,

$$\tilde{S}_{\alpha\beta}(kz) = \int d^3 p d^3 p' \tilde{S}(kz; \vec{p}\vec{p}') \quad (12)$$

in terms of the functions

$$\bar{J}_{\alpha\beta}(kz) = \int d\vec{p}d\vec{p}' \bar{J}_{\alpha\beta}(kz; \vec{p}\vec{p}') \quad (13)$$

where the $\bar{J}_{\alpha\beta}$'s are solutions to the simplified kinetic equations

$$\left(z - \frac{\vec{p} \cdot \vec{k}}{m\alpha}\right) \bar{J}_{\alpha\beta}(kz; \vec{p}\vec{p}') - \sum_{\gamma=e,1} \int d\vec{p}'' \phi_{\alpha\gamma}(kz; \vec{p}\vec{p}'') \bar{J}_{\gamma\beta}(kz; \vec{p}''\vec{p}') = M_{\alpha}(p) \delta(\vec{p}-\vec{p}') \delta_{\alpha\beta} \quad (14)$$

Specifically, the results for a system of electrons and ions are

$$\begin{aligned} \bar{S}_{ee}(kz) = & \frac{1}{E(kz)} [E_i(kz) (\bar{J}_{ee}(kz) S_{ee}(k) + \bar{J}_{ei}(kz) S_{ie}(k)) \\ & + (c_{ei}(k) - z(\bar{J}_{ee}(kz) c_{ei}(k) + \bar{J}_{ii}(kz) c_{ii}(k))) \\ & \times (\bar{J}_{ie}(kz) S_{ee}(k) + \bar{J}_{ii}(kz) S_{ie}(k))] \quad (15) \end{aligned}$$

and

$$\begin{aligned} \bar{S}_{ei}(kz) = & \frac{1}{E(kz)} [E_e(kz) (\bar{J}_{ii}(kz) S_{ie}(k) + \bar{J}_{ie}(kz) S_{ee}(k)) \\ & + (c_{ei}(k) - z(\bar{J}_{ii}(kz) c_{ie}(k) + \bar{J}_{ie}(kz) c_{ee}(k))) \\ & \times (\bar{J}_{ee}(kz) S_{ee}(k) + \bar{J}_{ei}(kz) S_{ie}(k))] \quad (16) \end{aligned}$$

where the functions $F_\alpha(kz)$ and $E(kz)$ are defined by

$$E_\alpha(kz) = 1 - c_{\alpha\alpha}(k) + z (\bar{J}_{\alpha\alpha}(kz) c_{\alpha\alpha}(k) + \bar{J}_{\alpha\beta}(kz) c_{\beta\alpha}(k)), \quad \alpha \neq \beta \quad (17)$$

$$E(kz) = E_e(kz) E_i(kz) - (c_{ei}(k) - z (\bar{J}_{ee} c_{ei}(k) + \bar{J}_{ei} c_{ii}(k))) \\ \times (c_{ie}(k) - z (\bar{J}_{ii} c_{ie}(k) + \bar{J}_{ie} c_{ee}(k))). \quad (18)$$

Various models for the collision operators will generate different approximations to the $\bar{J}_{\alpha\beta}$'s. Using these in Eqs (15-16), and their counterparts within the labels "e" and "i" interchanged will give estimates to the dynamic structure factors. These collision models will be studied in the next section.

III. THE COLLISION MODELS

In this section we will examine the charge-charge structure factors predicted by three different models for $\phi_{\alpha\beta}$ and compare them to the MD results of Ref. 8. All three models will require as input the direct correlation functions $c_{\alpha\beta}(k)$ which will be obtained from the solution to the two-component HNC equation with the potential in Eq. (1). The first and simplest model we will investigate is the collisionless or generalized Vlasov model in which $\phi_{\alpha\beta} = 0$. The second model employs a simple Fokker-Planck-like collision operator developed by Lenard and Bernstein²⁰. The final model is one suggested by Duderstadt and Akcasu²¹ which incorporates the exact high-frequency behavior of $\phi_{\alpha\beta}$ and models its time-dependence by simple exponential decay.

A. The Generalized Vlasov Model

In this model we simply neglect $\phi_{\alpha\beta}$ in Eq. (14) to obtain

$$\tilde{J}_{\alpha\beta}(kz) = \delta_{\alpha\beta} (1 + \chi_{\alpha}(kz)) / z ,$$

where

$$\chi_{\alpha}(k, z) = \int d^3p \frac{\vec{k} \cdot \vec{p} / m_{\alpha} M_{\alpha}(p)}{z - \vec{k} \cdot \vec{p} / m_{\alpha}} \quad (20)$$

is the plasma response function. Substituting Eq. (19) into Eq. (16) yields the usual RPA results for $\tilde{S}_{\alpha\beta}(kz)$ with one important difference. The results presented here contain the exact static correlation functions rather than their Debye-Huckel limits.

Taking these functions from HNC data, we calculated $S_{QQ}(k, \omega)$ for $\Gamma = 0.5$ and $r_s = 0.4$ for the same values of $q (=ka)$ used in the MD runs.⁸ The results are shown in Fig. 1 where the standard RPA curves are presented for comparison (the ordinate has been scaled by a factor of 100). It appears quite clear that even at the smaller values of the wavenumber q , where the collective modes will begin to exhibit evidence of dissipation not available in this collisionless model, that the generalized Vlasov results are in good agreement with the MD data.

Although this mean-field approximation may provide an adequate model of $S_{QQ}(k, \omega)$ for $\Gamma < 0.5$ (as long as q is ≥ 0.78), it does not give a good representation of the charge-charge spectrum at $\Gamma = 2$ unless q is restricted to much larger values. For appropriate comparison with MD results at this value of the coupling, we must introduce a reasonable approximation for $\phi_{\alpha\beta}$ in Eq.(14) and solve for $\tilde{J}_{\alpha\beta}$.

B. The Fokker-Planck Model

A simple model for $\phi_{\alpha\beta}$ that introduces an interparticle collision frequency, ν , and allows an analytic solution to Eq.(14) is²⁰

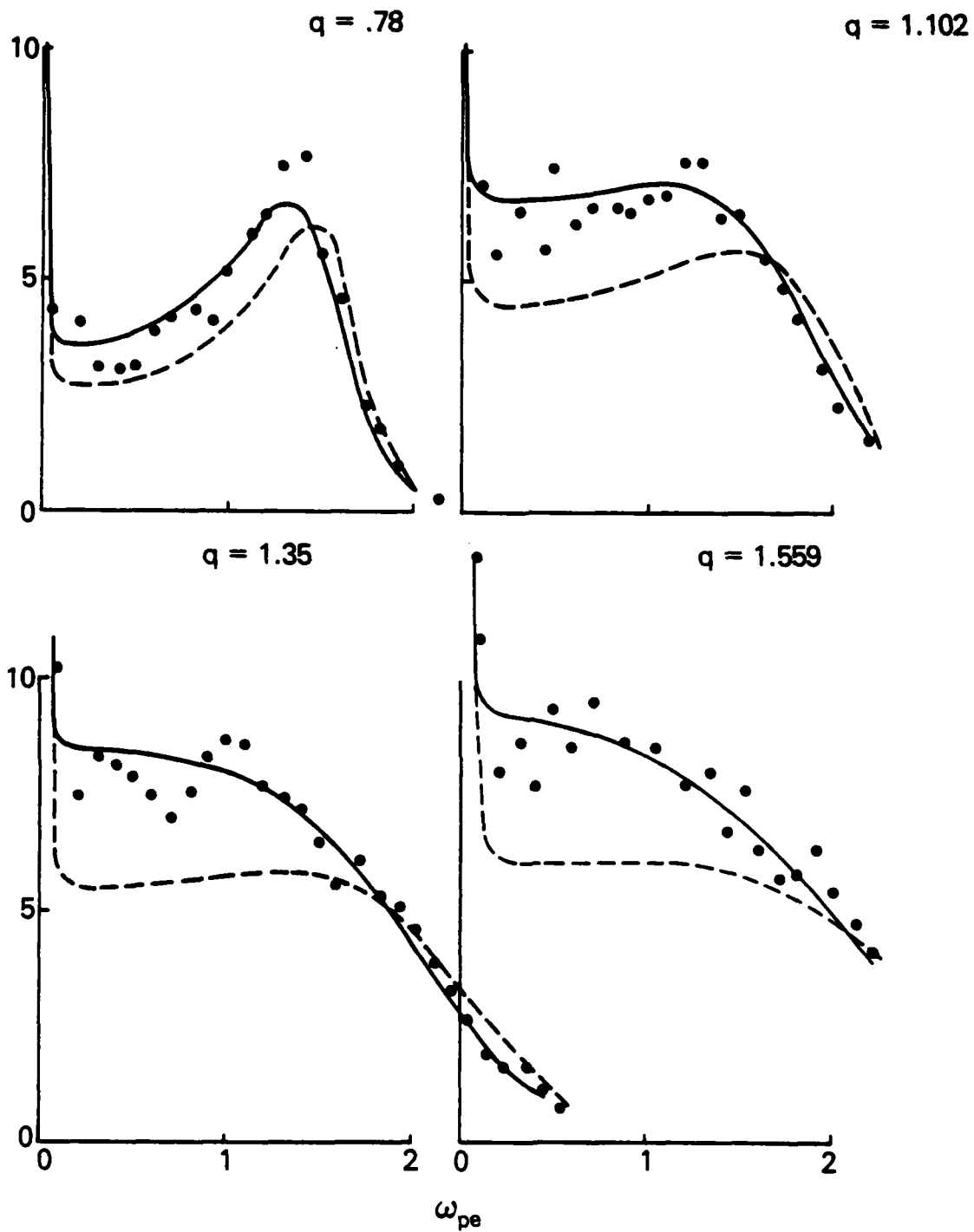


Figure 1

$S_{QQ}(k, \omega)$ ($\times 100$) as a function of ω/ω_{pe} for four values of $q = ka$ at $\Gamma = 0.5$ and $r_s = 0.4$. Dots: MD results. Dashed curve: Vlasov spectrum. Full curve: generalized Vlasov with HNC statics.

$$\Phi_{\alpha\beta}^{FP}(kz; \vec{p}\vec{p}') = i \frac{m_\alpha}{\beta} \delta_{\alpha\beta} v_{\alpha\beta} \frac{\partial}{\partial \vec{p}} \cdot \left(\frac{\partial}{\partial \vec{p}} + \frac{\beta}{m_\alpha} \vec{p} \right) \delta(\vec{p} - \vec{p}'). \quad (21)$$

Substituting this approximate collision term into Eq. (14) and Fourier transforming in momentum allows one to find ¹³

$$\bar{J}_{\alpha\beta}(kz) = \delta_{\alpha\beta} \check{K}_\alpha(kz), \quad (22)$$

where

$$\check{K}_\alpha(kz) = - (i\beta m_\alpha v_{\alpha\alpha} / k^2) I_\alpha(Q^2, s_\alpha - 1) \quad (23)$$

and

$$I_\alpha(Q^2, s_\alpha) = Q_\alpha^{-2} \frac{-2(Q_\alpha^2 + s_\alpha)}{Q_\alpha^2} e^{Q_\alpha^2} \int_0^{Q_\alpha^2} dx e^{-x} x^{(Q_\alpha^2 + s_\alpha)}. \quad (24)$$

In the above, $Q_\alpha^2 = k^2 / \beta m_\alpha v_{\alpha\alpha}^2$ and $s_\alpha = -iz / v_{\alpha\alpha}$.

Having introduced two collision frequencies, v_{ee} and v_{ii} , into our solution for $S_{QQ}(k, \omega)$ to allow for collisional damping, we must now select them with some care. It is well known that the ordinary Spitzer-like binary collision times are inappropriate in moderately to strongly coupled plasmas. We can, however, utilize transport coefficients found directly from the molecular dynamics simulations to obtain estimates of the required collision frequencies. In particular using the self-diffusion coefficients given by Hansen and McDonald⁸, these frequencies are seen to be

$$\frac{v_{ee}^{MD}}{\omega_{pe}} = \frac{1}{m_e \beta D_e} = \frac{1}{3\Gamma_e^*}$$

and

(25)

$$\frac{v_{ii}^{MD}}{\omega_{pe}} = \left(\frac{m_e}{m_i}\right)^{1/2} \frac{1}{3\Gamma_i^*}.$$

Collisions are found to be of negligible importance for $S_{QQ}(k, \omega)$ at $\Gamma = 0.5$. They are, however, necessary when describing $S_{QQ}(k, \omega)$ at larger values of coupling. In Fig. 2 we compare the collisionless generalized Vlasov model calculations (using "correct" HNC-evaluated direct correlation functions) with the results employing $v_{\alpha\alpha}^{MD}$ from Eq. (25) in the Fokker-Planck solution for the case $\Gamma = 2$, $r_s = 1$. From the figure it is clear that the model including collisions provides a much superior fit to the MD data than the collisionless model. For values of q smaller than 0.78, the discrepancy is still larger, indicating the failure of mean-field (RPA) descriptions of strongly coupled systems in the collective regime.

Even though the FP model considerably improves the shape of the spectrum, electron peak intensity for the FP curve, which is a sensitive function of $v_{\alpha\alpha}$, falls below the MD data points at peak. In addition the peak position is lower in frequency than is shown by the simulation. To correct this deficiency we must consider a different collision model.

C. Duderstadt Akcasu-Linnebur (DAL) Model

Neither of the first two models discussed above satisfy the third non-vanishing frequency moment of $S_{QQ}(k, \omega)$. This sum rule will however, be automatically satisfied by any model collision operator which incorporates the known high-frequency behavior of $\phi_{\alpha\beta}$. One such model is that suggested by Duderstadt and Akcasu²¹, and later applied to weakly coupled two-component plasmas by Linnebur and Duderstadt¹⁷, in which the time dependence of $\phi_{\alpha\beta}$ is modeled by two relaxation times. We define the DAL collision operator as

$$\begin{aligned} \phi_{\alpha\beta}^{DAL}(kz; \vec{p}\vec{p}') = & i \delta_{\alpha\beta} \frac{D_{\alpha}(0)}{z + i a_{\alpha}^s(k)} \frac{\partial}{\partial \vec{p}} \cdot \left(\frac{\partial}{\partial \vec{p}} + \frac{\beta}{m_{\alpha}} \vec{p} \right) \delta(\vec{p} - \vec{p}') \\ & + \frac{i}{z + i a_{\alpha\beta}^d(k)} M_{\alpha}(p) \vec{p} \cdot \vec{A}_{\alpha\beta}(k) \cdot \vec{p}' , \end{aligned} \quad (26)$$

where

$$D_{\alpha}(0) = D_{\alpha\alpha}(0) + D_{\alpha\beta}(0), \quad (\alpha \neq \beta) \quad (27)$$

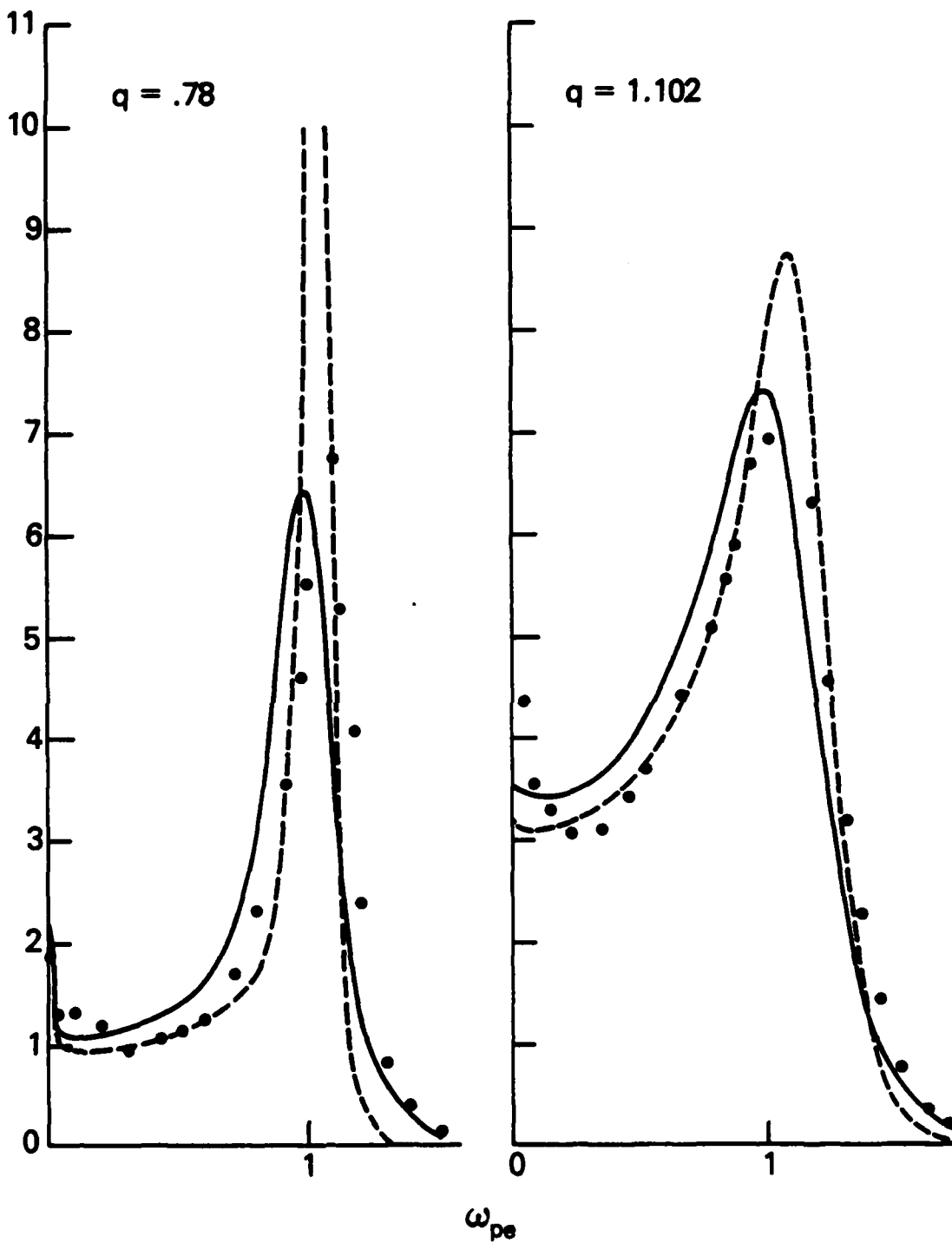


Figure 2

$S_{QQ}(k, \omega)$ for two values of q at $\Gamma = 2$, $r_s = 1$. Dots: MD results.
 Dashed curve: generalized Vlasov with HNC statics. Full curve: FP model.

$$D_{\alpha\beta}(0) = \frac{1}{3\beta} \int d\vec{r} g_{\alpha\beta}(r) v_{\alpha\beta}^2(r), \quad (28)$$

and

$$\bar{A}_{\alpha\beta}(k) = \frac{\hat{k}\hat{k}}{m_{\alpha}m_{\beta}} c_{\alpha\beta}(k) - \frac{\beta}{m_{\alpha}m_{\beta}} \int d\vec{r} g_{\alpha\beta}(r) e^{i\vec{k}\cdot\vec{r}} \hat{v}\hat{v}_{\alpha\beta}(r). \quad (29)$$

The decay constants $a_{\alpha\beta}^s(k)$ and $a_{\alpha\beta}^d(k)$ are chosen to obtain the correct short and long time, as well as the known large and small wave-number limits of $S_{\alpha\beta}(k, \omega)$.

Using Eq. (26) in Eq. (14) and once again Fourier transforming in momentum leads to

$$\bar{J}_{ee}(kz) = \frac{I_e(1 - iy_{ii} z m_i^2/k^2 \Delta_i) - im_e^2/k^2 y_{ee} \Delta_e + \frac{m_e^2 m_i^2}{k^4} z \Delta_e \Delta_i (y_{ei}^2 - y_{ee} y_{ii})}{1 - iy_{ii} z m_i^2/k^2 \Delta_i - iy_{ee} z m_e^2/k^2 \Delta_e + \frac{m_e^2 m_i^2}{k^4} z^2 \Delta_e \Delta_i (y_{ei}^2 - y_{ee} y_{ii})} \quad (30)$$

and

$$\bar{J}_{ei}(kz) = i \frac{\frac{m_e m_i}{k^2} y_{ei} \Delta_e \Delta_i}{1 - iy_{ii} z m_i^2/k^2 \Delta_i - iy_{ee} z m_e^2/k^2 \Delta_e + \frac{m_e^2 m_i^2}{k^4} z^2 \Delta_e \Delta_i (y_{ei}^2 - y_{ee} y_{ii})}, \quad (31)$$

where I_{α} is defined as in Eq. (23), but with $v_{\alpha\alpha}$ replaced by $w_{\alpha\alpha}(kz)$ which is given by

$$w_{\alpha\alpha}(kz) = \frac{\beta}{m_{\alpha}} \frac{D_{\alpha}(0)}{z + ia_{\alpha\alpha}^s(k)}. \quad (32)$$

The remaining functions appearing in Eq. (31) are

$$y_{\alpha\beta}(kz) \equiv \frac{1}{z + ia_{\alpha\beta}^d(k)} \hat{k} \cdot \bar{A}_{\alpha\beta}(k) \cdot \hat{k} \quad (33)$$

and

$$\Delta_{\alpha} \equiv zI_{\alpha}^{-1} . \quad (34)$$

The form of the damping functions are chosen to be

$$a_{\alpha\beta}^{s,d}(k) = a_{\alpha\beta}(0) [1 + (k/k_{\alpha\beta}^{s,d})^2] , \quad (35)$$

where the unknown parameters $a_{\alpha\beta}(0)$ and $k_{\alpha\beta}^{s,d}$ are determined from known k and ω constraints on $S_{\alpha\beta}(k, \omega)$.^{21,22} With these restrictions we are required to choose only two other collision frequencies to complete the description of the DAL model. Those coefficients are the electron-ion and ion-electron collision frequencies, ν_{ei} and ν_{ie} , characterizing momentum transfer between particles.

We can find ν_{ei} from the coefficient of electrical conductivity provided by the MD data,

$$\frac{\nu_{ei}^{MD}}{\omega_{pe}} = \frac{\omega_{pe}}{4\pi\sigma} = \frac{1}{4\pi\sigma^*} . \quad (36)$$

As an alternative to using the simulation derived conductivity to find ν_{ei} , we can employ a quantum kinetic theory treatment of plasma time-correlation functions²³ which leads directly to the calculation of the electrical conductivity.²⁴ This treatment can be thought of as a quantum generalization of the fully renormalized kinetic theory of Mazenko¹⁵ in which the disconnected approximation (DA) is used to renormalize the potential terms in the collision operator. The application of this approximation to strongly coupled plasmas has been discussed in Ref. 22 and elsewhere.^{25,26} More recently the theory has led to numerical evaluations of σ (or ν_{ei} , which we label ν_{ei}^{DA}) for the cases under consideration here.²⁷ We can estimate ν_{ee}^{DA} by taking

$$\nu_{ee}^{DA} = \frac{\nu_{ee}^{MD}}{\nu_{ei}^{MD}} \nu_{ei}^{DA} .$$

The collision frequencies are collected in Table I for the cases used in the simulation runs. The results employing the DAL model with MD and DA collision frequencies for a $\Gamma = 2$, $r_s = 1$ TCP are given in Fig. 3. At low

Table I

Collision frequencies (in units of ω_{pe}) derived from molecular dynamics transports coefficients (MD - Eqs. (25) and (36)) and calculated from the disconnected approximation (DA - Ref. 27, Eq. (41)).

	$\Gamma = 0.5$ $r_s = 0.4$	$\Gamma = 0.5$ $r_s = 1$	$\Gamma = 2$ $r_s = 1$
MD ν_{ee}	0.054	0.093	0.135
DA ν_{ee}	0.111	0.225	0.201
MD ν_{ei}	0.022	0.037	0.073
DA ν_{ei}	0.045	0.090	0.109

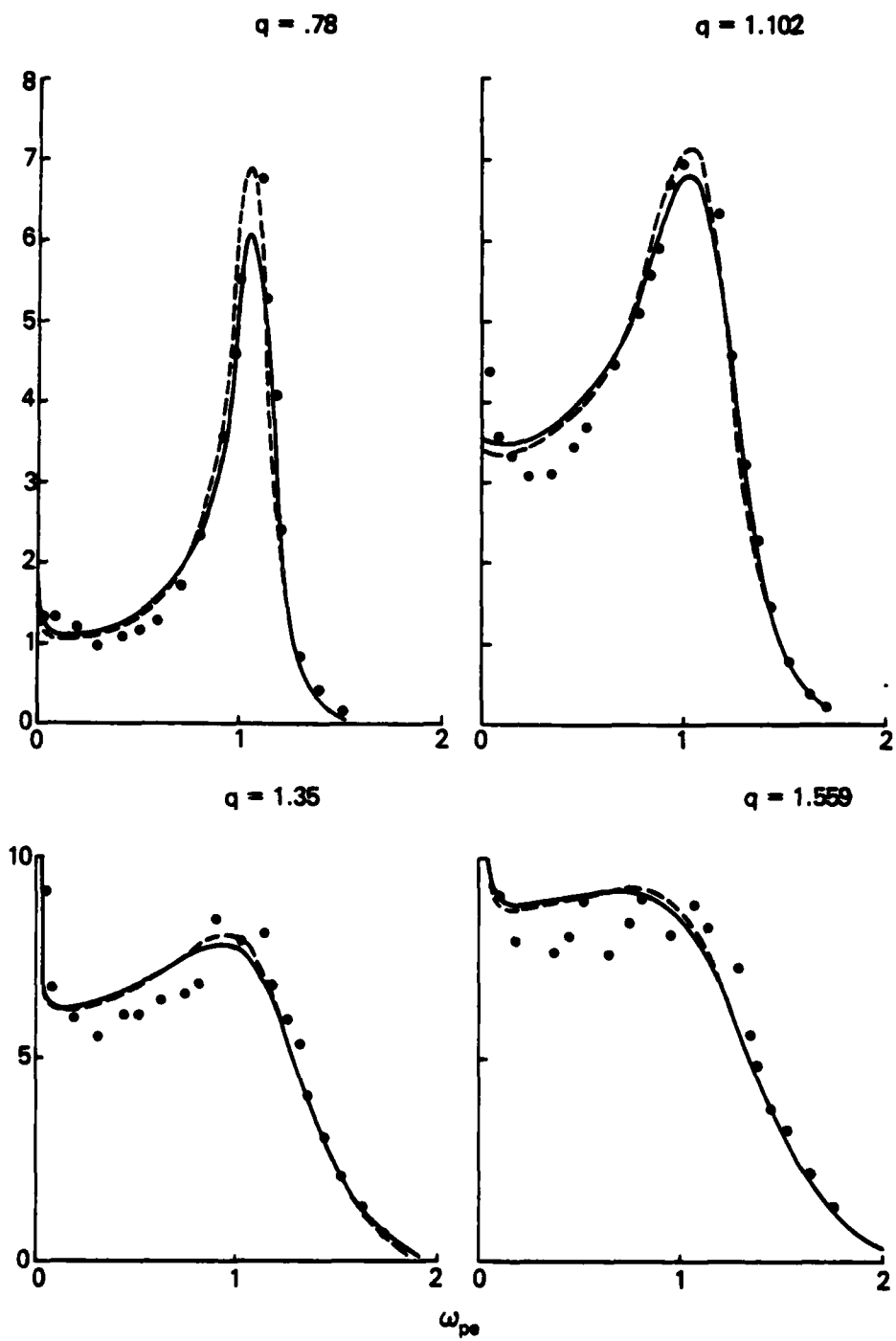


Figure 3

$S_{QQ}(k, \omega)$ for four values of q at $\Gamma = 2$, $r_s = 1$. Dots: MD results. Curves are DAL model results with $\nu = \nu^{DA}$ (dashes) and $\nu = \nu^{MD}$ (full).

k , it is apparent that the fits are superior to the FP model in peak position as well as the intensity of the resonance. At small wavelengths the generalized Vlasov solution is nearly identical with those of the collision models, indicating the lack of importance of collisions in this regime.

In their paper, Hansen and McDonald⁸ developed a memory function theory (mft) based on the work of Abramo, et al.²⁸ to describe the charge-fluctuation spectra obtained in the MD simulations. This theory builds a hierarchy of memory functions for linear combinations of momentum-integrated microscopic particle densities defined in terms of known sum rules. The hierarchy is truncated at the highest order in which the sum rules can be exactly calculated using two-particle radial distribution functions (the fourth order sum rule). The highest order memory functions are damped in time by an exponential or Gaussian approximation employing relaxation times defined, again, by the known sum rules.

The advantage of "mft" lies in the fact that only two relaxation times are required and that these constants are determined within the framework sum rule calculations. The DAL model on the other hand, requires the determination of four independent relaxation times by introducing four transport coefficients. However, since these time constants interpolate between hydrodynamic and Vlasov behavior, a knowledge of the needed transport coefficients (which can be accurately found from MD simulations or quantum kinetic theory) ensures correct small k , small ω limits of $S_{QQ}(k, \omega)$. The charge-fluctuation spectra predicted by the DAL model and mft are very similar for all of the cases under consideration here (see Figs. 6 and 8 of Ref. 8). Results of $S_{\alpha\alpha}(k, \omega = 0)$ for these models are collected in Table II.

As noted above, one may expect differences to occur at longer wavelengths where the DAL model has used transport coefficients to ensure correct hydrodynamic behavior. In Fig. 4 we present a comparison of mft with the DAL model using values of the collision frequencies obtained from MD transport coefficients and the quantum theoretical treatment with the disconnected approximation at $q = 0.307$. The mft results were taken from Figs. 9 and 10 of Ref. 8. The DAL model using v^{MD} predicts a plasma peak of greater intensity and lower frequency than the mft calculations. The

Table II

$S_{QQ}(k, \omega = 0)$ for Duderstadt-Akcasu-Linnebur interpolation model (DAL), Fokker-Planck collision model (FP), and generalized Vlasov (GV) and Vlasov (V) collisionless models compared with memory function theory (mft) and MD simulation data. $\nu_{\alpha\beta}^{MD}$ was used in the DAL and FP calculations.

$$S_{QQ}(k, \omega = 0)$$

q	$\Gamma = 0.5 \quad r_g = 0.4$					$\Gamma = 0.5 \quad r_g = 1$					$\Gamma = 2 \quad r_g = 1$							
	MD	mft	DAL	FP	GV	V	MD	mft	DAL	FP	GV	V	MD	mft	DAL	FP	GV	V
0.78	0.26	0.32	0.31	0.31	0.31	0.39	0.33	0.40	0.35	0.36	0.35	0.39	0.02	0.025	0.022	0.022	0.021	0.064
1.10	0.86	0.79	0.78	0.78	0.77	0.80	0.85	0.83	0.79	0.79	0.78	0.80	0.07	0.045	0.036	0.036	0.033	0.16
1.35	1.20	1.26	1.21	1.23	1.21	1.17	1.28	1.22	1.18	1.18	1.16	1.17	0.21	0.15	0.13	0.12	0.12	0.29
1.56	1.45	1.60	1.59	1.60	1.58	1.38	1.80	1.51	1.48	1.48	1.45	1.38	0.40	0.32	0.29	0.29	0.29	0.39

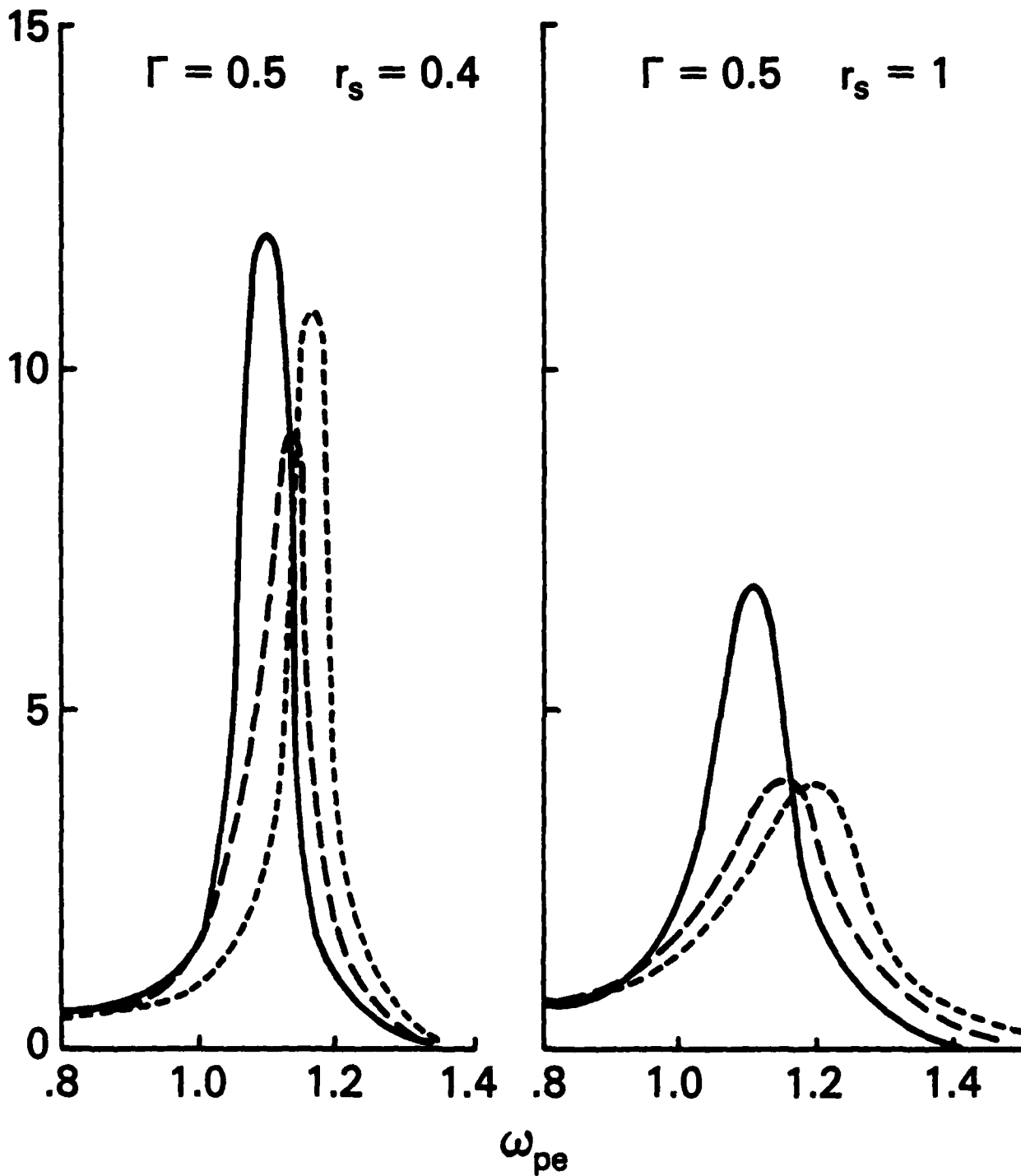


Figure 4

Comparison of model results at $\Gamma = 0.5$, $r_s = 0.4$ for $q = 0.307$ Dotted curve: mft results of Hansen and McDonald. Dashed curve: DAL model with $\nu = \nu^{DA}$. Full curve: DAL model with $\nu = \nu^{MD}$.

DAL model using the larger values of ν^{DA} predicts a smaller intensity and a peak position closer to mft. Differences between these theoretical approaches can be expected to increase as q is made smaller still. Unfortunately there are no MD results at these wavenumbers to indicate which is the preferable theoretical prediction.

IV. DISCUSSION

The collision approximations we have investigated for describing the TCP all utilize equilibrium correlation data as input to the solutions. This data has been shown⁸ to be accurate and easily obtained from the solution of the hypernetted chain integral equations using the Deutsch potential as the effective interparticle interaction potential. We have used this data in all models considered with the exception of the usual Vlasov approximation.

As has already been shown⁸, the standard Vlasov equation, which contains neither collisional dynamics nor correct initial time correlation information, does not reproduce any of the MD spectra accurately. The generalized Vlasov equation, in which the Fourier transform of the potential in the mean-field term is replaced by the exact direct correlation function, provides a reasonable fit to the data at $\Gamma = 0.5$ for all r_g and q values simulated. This approximation is also adequate for large wavenumbers at higher values of the coupling parameter.

At the higher value of Γ considered here, it is necessary to include collisions in order to damp the strongly spiking plasmon peak. The Fokker-Planck-like Lenard-Bernstein model approximates these effects by introducing two self-collision times into the solution of $S_{QQ}(k, \omega)$. Even though these constants are well-known, the resulting spectra are only qualitatively similar to the MD data at smaller values of q . As we have noted, the FP term does not satisfy the fourth frequency moment sum rule. In addition the collisional invariant of momentum is not satisfied by this model.²⁹

The DAL model does incorporate exact sum rules up to fourth order and does satisfy conservation of momentum, leading to much improved results at low q in the case of large coupling.³⁰ The implementation of several relaxation times allows the collision dynamics to be interpolated from

known hydrodynamic ($k \rightarrow 0$, $\omega \rightarrow 0$) forms of $S_{\alpha\beta}(k, \omega)$ to their Vlasov and free particle forms. This approximate form of the collision term depends on the accuracy of the acquired hydrodynamic coefficients, but is seen here to give a good description of the MD charge-fluctuation spectra. This description is very similar to the mft calculations except at low wavenumber where the interpolative DAL model should represent the spectra resonances as accurately as the transport coefficients provided. For all cases $\Gamma \leq 2$ and $q \geq 0.78$, the distinctions are negligible.

The primary limitation in this process is the accurate calculation of the radial distribution functions from the HNC procedure. This implies that the best solutions will arise from the most inclusive effective interionic potential. The Deutsch potential, Eq. (1), is not valid for Γ greater than about two, but the HNC scheme should give reasonable distribution functions for a more general effective potential. From these functions relaxation times can be derived and used in the DAL collision term to provide accurate predictions of dynamic correlation functions in more strongly coupled two-component plasmas over a wide range of k and ω .

Acknowledgments

The authors would like to thank Prof. Hansen for providing data from the molecular dynamics simulation runs. The work of one of us (D.B.B.) was done under the auspices of the U.S. Department of Energy by Lawrence Livermore National Laboratory under Contract No. W-7405-Eng-48. This work was supported in part by the Office of Naval Research.

References

1. S. G. Brush, H. L. Sahlín, and E. Teller, J. Chem. Phys. 45, 2102 (1966).
2. J. P. Hansen, Phys. Rev. A8, 3096 (1973); P. Vieillefosse and J. P. Hansen, Phys. Rev. A12, 1106 (1975) and references cited therein.
3. J. P. Hansen, I. R. McDonald, and E. L. Pollock, Phys. Rev. A11, 1025 (1975).
4. M. Baus and J. P. Hansen, Phys. Rep. 59, 1 (1980).
5. S. Ichimaru, Rev. Mod. Phys. 54, 1017 (1982).
6. C. Deutsch, Phys. Lett. 60A, 317 (1977).
7. J. P. Hansen and I. R. McDonald, Phys. Rev. Lett. 41, 1379 (1978).
8. J. P. Hansen and I. R. McDonald, Phys. Rev. A23, 2041 (1981).
9. R. Cauble and J. J. Duderstadt, Phys. Rev. A23, 3182 (1981).
10. A. Z. Akcasu and J. J. Duderstadt, Phys. Rev. 188, 479 (1969).
11. R. Zwanzig, Lectures in Theoretical Physics, V. 3 ed. W. E. Brittin, B. W. Downs and J. Downs, (Wiley, New York, 1961). p. 106
12. H. Mori, Prog. Th. Phys. (Kyoto) 33, 423 (1965).
13. J. L. Lebowitz, J. K. Percus, and J. Sykes, Phys. Rev. 188, 487 (1969).
14. E. P. Gross, Ann. Phys. 69, 42 (1972).
15. G. F. Mazenko. Phys. Rev. A9, 360 (1974).
16. D. Forster and P. Martin, Phys. Rev. A5, 1575 (1975).
17. E. Linnebur and J. J. Duderstadt, Phys. Fluids 16, 665 (1973).
18. J. F. Springer, M. A. Pokrant, and F. A. Stevens, Jr., J. Chem. Phys. 58, 4863 (1973).
19. K. C. Ng, J. Chem. Phys. 61, 2680 (1974).
20. A. Lenard and I. B. Bernstein, Phys. Rev. 112, 1456 (1958).
21. J. J. Duderstadt and A. Z. Akcasu, Phys. Rev. A2, 1097 (1970).
22. A. Z. Akcasu and E. L. Linnebur, Neutron Inelastic Scattering (IAEA, Vienna, 1972).
23. D. B. Boercker and J. W. Dufty, Phys. Rev. A23, 1952 (1981).
24. D. B. Boercker. Phys. Rev. A23, 1969 (1981).
25. H. Gould and G. F. Mazenko, Phys. Rev. A15, 1274 (1977).
26. T. Wallenborn and M. Baus, Phys. Rev. A18, 1737 (1978).
27. D. B. Boercker, F. J. Rogers, and H. E. DeWitt, Phys. Rev. A25, 1623 (1982).

28. M. C. Abramo, M. Parrinello, and M. P. Tosi, J. Phys. C. 7, 4201 (1974).
29. See e.g., D. Forster, Phys. Rev. A9, 943 (1974).
30. In the OCP, see, e.g., Fig. 5 of Ref. 9.

DATE
ILME